DYNAMIC MORPHOLOGY OF CALCIUM-INDUCED INTERACTIONS BETWEEN PHOSPHATIDYLSERINE VESICLES

R. P. RAND, B. KACHAR, AND T. S. REESE
Department of Biological Sciences, Brock University, St. Catharines, Ontario, Canada L2S 3A1; and Laboratory of Neurobiology, National Institutes of Neurological and Communicative Disorders and Stroke, National Institutes of Health, Bethesda, Maryland 20205

ABSTRACT Structural changes in phosphatidylserine vesicles exposed to calcium chloride for various times have been observed by means of video-enhanced light microscopy and freeze-fracture electron microscopy. Large flat double-bilayer diaphragms form at the contacts between aggregated vesicles within milliseconds. Bilayers at and outside of diaphragms rupture and allow vesicles to collapse completely by flattening against each other within seconds. Collapse through intermediate states to a stable multilamellar phase is complete within minutes. The Ca-induced attraction energy and the resultant flattening at contacts between vesicles is far beyond that needed to stress bilayers to the point of rupture. Although the destabilizing response to this stress is preferential to the diaphragm region, 40% of adhering pairs rupture outside of the diaphragm region rather than fuse with each other. In this respect the mechanism of fusion between these vesicles may be fundamentally different from the controlled fusion process in cells.

INTRODUCTION

Calcium-induced secretion by exocytosis occurs in many types of cell and typically depends on the leakless fusion of membrane-bound intracellular vesicles with the plasma membrane (1–4). We use the term fusion to mean the topological changes that require as a minimum two critical steps; (*a*) very close approach of the two membranes, and (*b*) destabilization, rupture, and joining of the two membranes only in the contact area. Studies of artificial bilayer membranes have taught us the requirements for close enough approach for fusion (5). However, the second step is difficult to capture because it appears to be rapid and limited to a small area of the contacting membranes (2, 4). The complexity of cell membranes makes it even more difficult to attribute the mechanism of either of these two steps to particular membrane components. Consequently, protein-free phospholipid bilayers continue to be widely used as models of membrane interactions and fusion.

For model systems to shed light on mechanisms relevant to the cellular process it is important to establish that they at least mimic the topology of leakless fusion. A technique particularly designed to assess this (6) measures Ca-induced vesicle aggregation (by light scattering), mixing of the internal contents of interacting vesicles (by terbium-dipicolinic fluorescence), and leakage of the vesicle contents to the medium (by release of carboxyfluorescence quenching). An important conclusion from these studies (and others on a wide variety of lipid systems [7]) is that fusion, when it occurs, is the first very rapid reaction upon vesicle contact. With few exceptions this is closely followed by vesicle rupture and collapse with the formation of bulk lipid phases. The only stage in these model systems that appears relevant to the cellular process is that which occurs immediately after the initial vesicle contact (7). Questions remain (24) as to whether the fusion reaction and vesicle rupture are clearly sequential enough in time for the processes to be independent of each other.

One model system that has received considerable attention is the response of phosphatidylserine (PS) vesicles to added divalent cations. The major barrier to very close approach of all bilayer membranes is a ubiquitous hydration repulsion (5). It derives from having to dehydrate hydrophilic groups and likely dominates close interaction of all hydrophilic surfaces (5). Calcium dehydrates PS bilayers and promotes their close apposition (8, 9, 10). The second step, which itself may depend on dehydration, must involve a major structural perturbation of bilayer structure. Major perturbations have been observed in pure phospholipid bilayers with the discovery of pits and particles on their surface (11). However, they have been observed only as equilibrium structures in interacting bilayers that contain lipids conducive to assembling into nonbilayer arrangements. Their structure has been variously interpreted (11–15) in models of bilayer fusion. However, PS has never been observed to assemble into any nonbilayer structure. Therefore the perturbations seen as pits and particles in other lipid systems either are not relevant to the mechanism of PS vesicle fusion or exist only transiently in the PS systems during vesicle interaction.

Recently Miller et al. (16) have used freeze fracture to observe the effects of Ca on small sonicated unilamellar vesicles; vesicles that, as anticipated (23), do leak during fusion (7). They detected, within 10 ms after mixing, not only twinned vesicles but also flattened vesicles and multilayers; the sequence of structural changes remained unclear.

We have attempted to look at the intermediates in the interaction of large PS vesicles by asking the following questions relevant to fusion: (*a*) what is the nature of the initial Ca-induced contact between vesicles and can bilayer destabilizations be detected? (*b*) what is the reaction of the vesicles to that contact? (*c*) what is the product of that reaction? We have used two direct approaches. The first is to observe interacting vesicles by video-enhanced differential interference contrast light microscopy (17, 18). The second is to combine rapid mixing of $CaCl_2$ and PS vesicles with freeze-fracture electron microscopy.

MATERIALS AND METHODS

Lipid and Vesicle Preparation

Bovine brain PS was obtained from Avanti Polar Lipids, Inc. (Birmingham, AL). X-ray diffraction results of the lipid behavior in water indicates that it contains divalent cations. It was converted to the Na salt using a chloroform-methanol aqueous two-phase system. Subsequent thin-layer chromatography showed the lipid to be >99% pure, and it was stored dry under nitrogen at −60°C.

Giant complex vesicles (GCV) were produced by overnight hydration of 10 mg PS in 10 ml, 2 mM TES buffer (pH 7.4) followed by vortexing until a visibly uniform suspension was observed. We have called these GCV because they are several microns in diameter, are usually oligolamellar, and contain several small freely diffusing vesicles. Large unilamellar vesicles (LUV) were formed by the reverse evaporation phase method of Sozka et al. (19) using 10 mg lipid/ml. The final sizing was done by filtering through a 0.1-μm Nucleopore membrane.

Rapid Mixing, Spray-Freezing, Freeze-Fracture Electron Microscopy

Rapid spray freezing of LUV and GCV without cryoprotectant was done on standard Balzers equipment (Balzers, Hudson, NH). However, before freezing the vesicle suspension was very rapidly mixed (milliseconds) with an equal volume of a second solution using a Berger ball mixer (Commonwealth Technology, Inc., Alexandria, VA), as shown in Fig. 1. The second solution contained various concentrations of $CaCl_2$ in the vesicle medium. Freezing was accomplished at a series of intervals down to ~100 ms after mixing. The freeze fracturing and replicating were done in a standard manner on Balzers equipment.

Video-enhanced Differential Interference Contrast Microscopy

For the light microscopic observations, a solution of GCV was placed on a shallow chamber between a microscopic slide and a coverslip. $CaCl_2$ was added by placing a small concentrated drop (10–100 mM) through a side opening. Preparations were observed with a Zeiss ICM inverted microscope (Carl Zeiss, Inc., Thornwood, NY) equipped for differential interference contrast (DIC), with an oil immersion 1.4 NA condenser and 1.3 NA plan APO 100× objective. A dramatic improvement in the performance of the DIC microscope is obtained when the image is viewed with a high-resolution video system (18). The video camera was a C-1000 Chalnicon camera driven by a polyprocessor frame memory (Hamamatsu Systems, Inc., Waltham, MA). At high video gains a mottle pattern appeared in the background due to unavoidable dirt and imperfections in the lenses (18). The frame memory was used to subtract this pattern continuously from succeeding frames. The magnification of the images seen on a 19 in. monitor was 10,000× and represented an optical section ~0.2 μm thick.

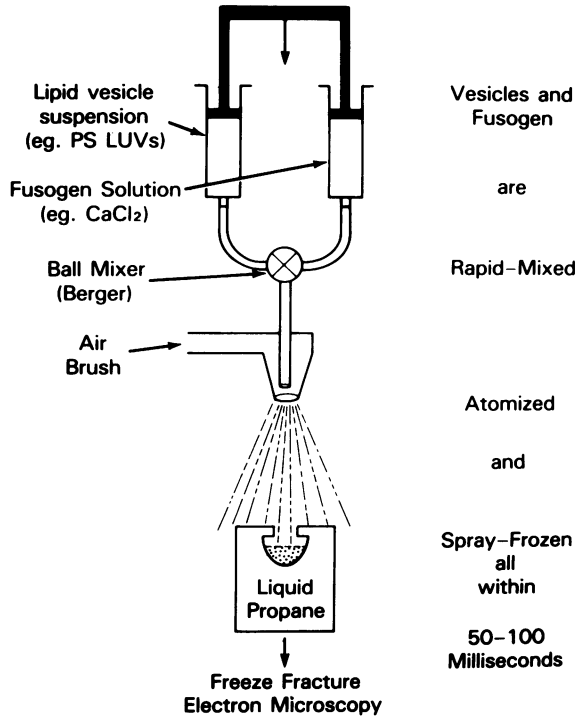

FIGURE 1 Schematic diagram of the method of rapid mixing and rapid freezing. Mixing is complete within a few milliseconds. The minimum time to freezing thereafter is determined by the time of flight of the atomized droplets, estimated visually. The important time with respect to the vesicle morphology is the uncontrollable time of vesicle collision after mixing with the $CaCl_2$ solution.

RESULTS

Video-enhanced Light Microscopy

Observations in many experiments revealed that on $CaCl_2$ addition all vesicles rupture and the final state consisted of highly condensed optically dense lipid fragments. The optical section was so thin and some events so fast that not all topological changes during the process could be defined. Where it could, and with frame by frame analysis, we established that the following sequence of changes occurs as the wave of $CaCl_2$ passes through the GCV suspension. Contacting oligolamellar spherical vesicles, after variable delays, rapidly form a flat area of contact that can persist for several seconds. One of two events ensues. The diaphragm so formed eventually ruptures to form a single vesicle that encloses the contents of both original vesicles (Fig. 2; *a–c*). No $CaCl_2$ appears to enter the vesicle interior because no further changes occur internally. Alternatively, one of the outer portions of adhering vesicles ruptures and

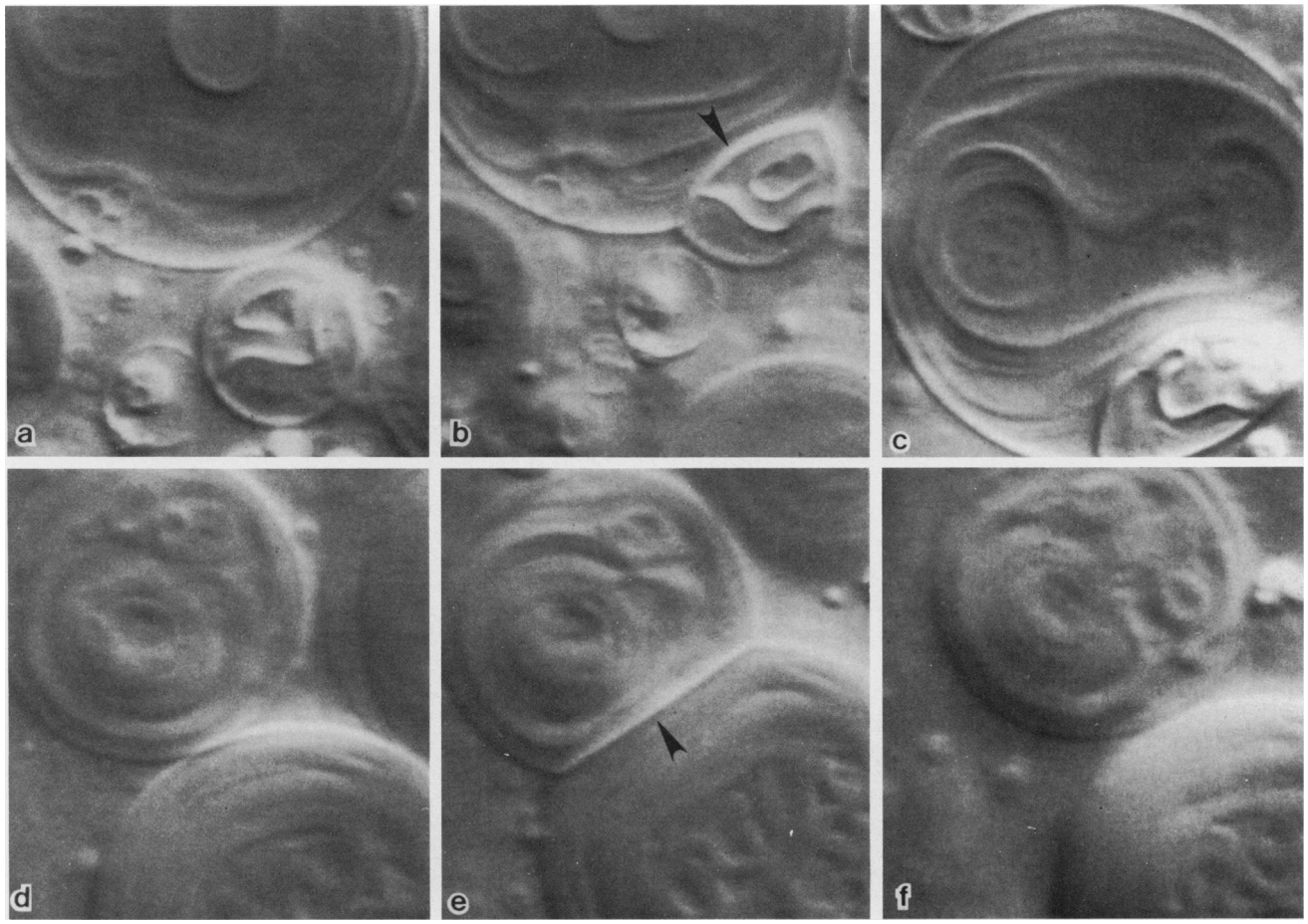

FIGURE 2 Still frames of video-enhanced differential interference contrast images of Ca-induced interactions between giant multilamellar PS vesicles. Contacting spherical vesicles (*a* and *d*) form flat areas of contact after a variable time delay (arrowheads in bands *b* and *e*) that persist for several seconds. The resulting diaphragm can rupture and the contents of the two vesicles mingle (*c*), or one of the outer portions of adhering vesicles can rupture releasing its contents and letting it move away from the other vesicle (*f*). *a–c*, × 4,000; *d–f*, × 5,000.

disappears within one video frame (17 ms), leaving the two vesicles free to jump apart (Fig.2; *d–f*). What becomes of the ruptured outer lamella was difficult to discern. Single nonadhering vesicles also ruptured; we attribute this to undetected small vesicles adhering to a larger vesicle leading to the rupture of its outer bilayer. These three processes are speeded up at higher $CaCl_2$ concentrations. Out of 30 ruptures of adhering vesicles, 18 (60%) involved diaphragms, and 12 (40%) occurred in the extra-diaphragm portion of the vesicle. Since the diaphragm area is smaller than the extra-diaphragm area, the probability of a unit area of diaphragm rupturing is >60%. Using both the relative surface area of diaphragms, typically shown in Fig. 2 *e*, and the observed probabilities of rupture we estimate that the probability of a unit area of bilayer rupturing is ~10 times greater in the diaphragm area than outside it.

Freeze Fracture

Two major stages were identified in the transition between the equilibrium morphologies of the isolated vesicles and of the collapsed Ca-PS multilamellar phase. The two equilibrium states and the two transition states are described below.

Control LUV and GCV appear as isolated, smooth-surfaced spheres whether or not they were mixed with Ca-free solution. Their isolation is indicative of their high net surface charge, particularly evident in cross-fractured GCV, many of which contain a number of smaller vesicles that appear to maximize their mutual separation. Their spherical shape indicates that any effects of shear stresses involved in the rapid mixing and atomization of the vesicle suspension are not maintained. Large dilution of vesicles on mixing with the $CaCl_2$ solutions, so that vesicle contact was precluded before freezing, results in vesicles whose appearance is indistinguishable from the control. This indicates that any effects of $CaCl_2$ asymmetry of osmotic imbalance is not detectable within several seconds after mixing.

The structure in freeze fracture of the final collapsed multilamellar phase has already been adequately described (20). It is clear that a large number of vesicles contribute to

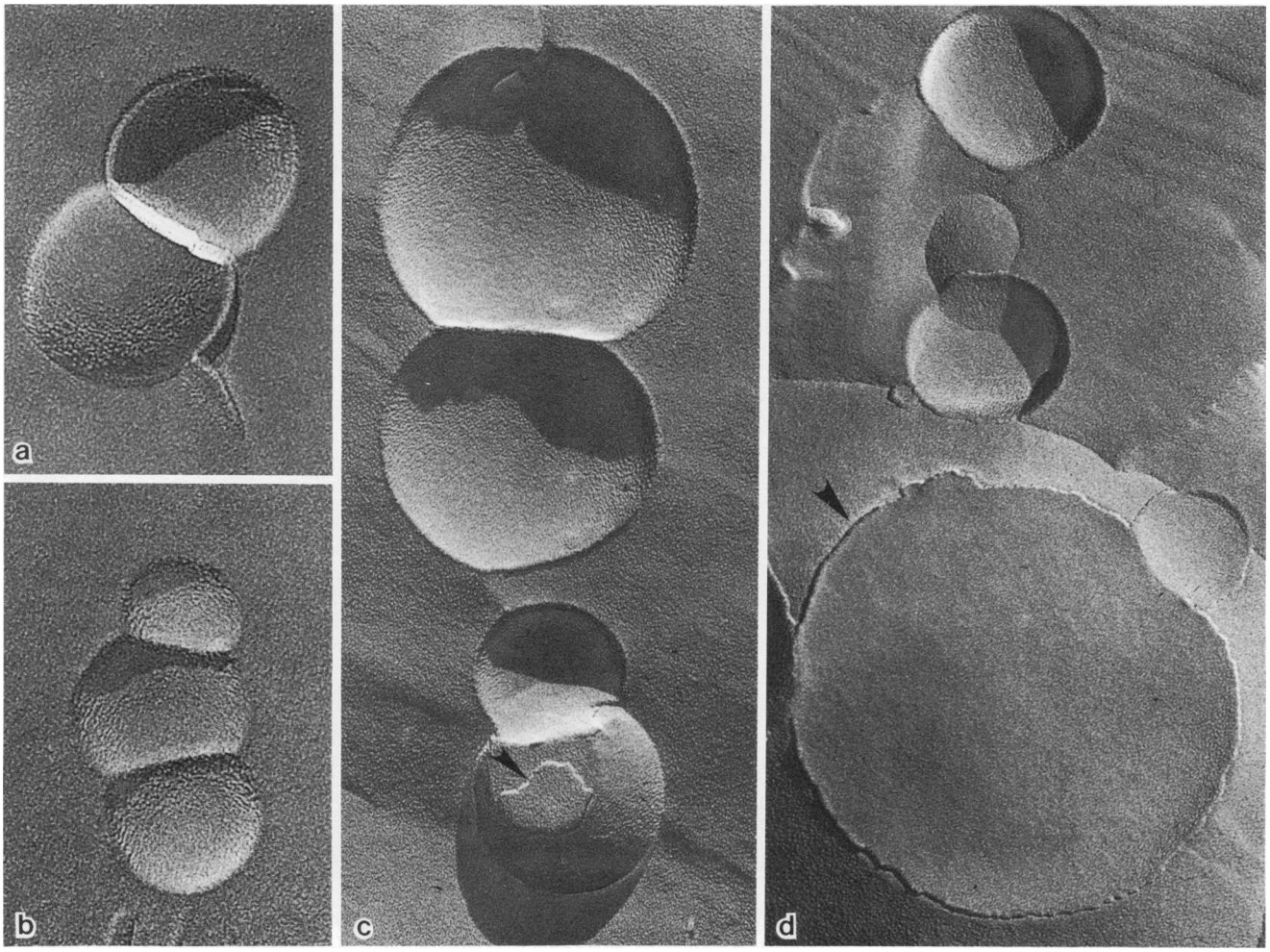

FIGURE 3 Freeze fracture of fast-frozen, rapid-mixed PS (LUV, *a–c*; GCV, *d*) vesicles showing the earliest observed changes (<100 ms) after addition of 5 mM $CaCl_2$. Aggregation of two (*a*) or more (*b–d*) vesicles produces large, flat diaphragms at the area of contact (*c* and *d*). All diaphragms appear to be made up of two tightly apposed bilayers (arrowheads in *c* and *d*). *a,b*, × 160,000; *c*, × 130,000, and *d*, × 110,000.

these large aggregates of bilayer stacks. That these were the collapsed PS-Ca dehydrated phase (8, 10) was confirmed by x-ray diffraction of a portion of the rapid-mixed sample.

Early Transition Morphology. Vesicle aggregation with the formation of smooth flat diaphragms in the areas of contact was the earliest change found in LUV (Fig. 3; *a–c*) and GCV (Fig. 3 *d*) at ~100 ms after addition of 5 mM $CaCl_2$. Thus a spherical vesicle acquires a flat side regardless of any disparities in size of the vesicle pair. Although LUV vary considerably in size, there was no obvious change in size at this stage after the addition of $CaCl_2$. Contact areas appear in all instances to be double-bilayer diaphragms. Isolated vesicles were all spherical in shape.

Later Transition Morphology. The next recognizable transition state was morphologically quite complex (Fig. 4) and found with increasing frequency after adding 5 mM $CaCl_2$. It is characterized by high curvature ridges or grooves on the cleaved surfaces of large aggregates of highly deformed and apparently collapsing or fusing vesicles. One remarkable feature of these ridges is their width, ~50 nm. These ridges are interpreted as edges of diaphragms of nearly collapsed vesicles (see Fig. 5). In many of the multiple arrays of ridges, their width is significantly less (20 nm; Fig. 4 *b*). The length of ridges in the multiple arrays is also remarkably uniform (Fig. 4; *b–e*). This uniformity indicates that they cannot be simply collapsed aggregates of vesicles since these would be of differing size. Cross fractures and surface views show the interior of these stacks to be multilamellar (Fig. 4 *d*).

No other morphological states could be discerned in photographs of several hundred microscopic fields. Either at intermediate times (30 s) after rapid mixing at lower $CaCl_2$ concentrations (2.5 mM), or at the shortest times at higher $CaCl_2$ concentrations (10 mM), images of the two

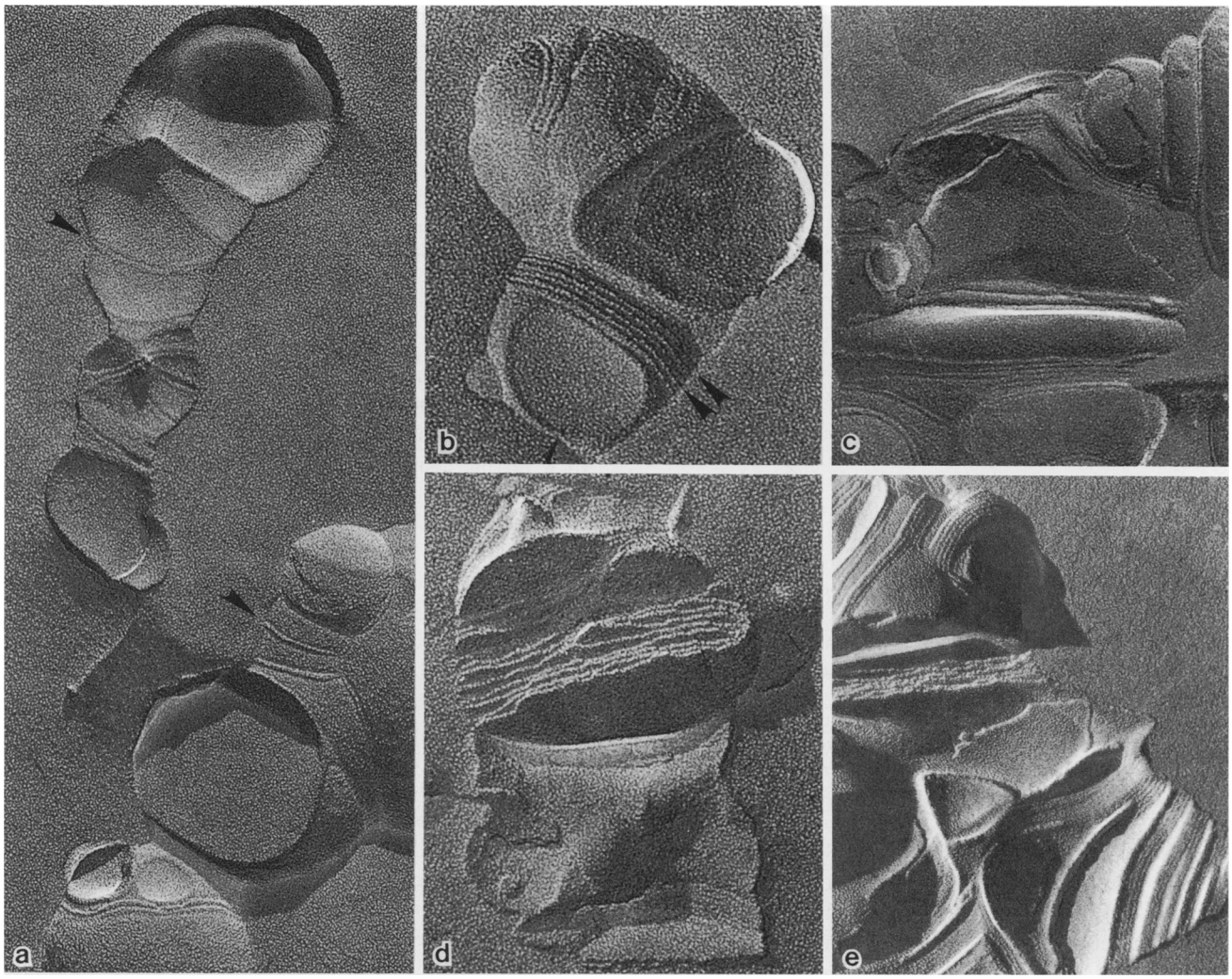

FIGURE 4 Later stages of vesicle interaction (30 s) showing high curvature ridges or grooves (50 nm diameter) on the surfaces of highly deformed and apparently collapsing vesicles (arrowheads in *a*). Arrays of uniform ridges 20 nm in diameter are also present on some vesicle aggregates (arrowheads in *b*). Cross fractures through aggregates (*d* and *e*) show that the interior of these stacks is multilamellar. *a*, *c–e*, × 135,000; *b*, × 160,000.

transient states coexist. Thus at higher concentrations of $CaCl_2$ the same sequence of changes occur but proceed at a faster rate.

DISCUSSION

The Ca-induced changes in morphology of the interacting vesicles could not be synchronized completely because starting time depends on vesicle collision. Thus images obtained 100 ms after mixing represent times of vesicle contact up to a maximum of 100 ms. Nevertheless, all images fall into one of the four categories described. Any other intermediate states must be so short lived as to make their detection, with the present level of sampling, highly improbable.

Our interpretation of the morphological changes induced by $CaCl_2$ is as follows. Flat double-bilayer diaphragms form within 100 ms after addition of $CaCl_2$, resulting in aggregation of from two to many contacting vesicles. Nondiaphragm regions are portions of a sphere similar in size to the original vesicles. No pairs, triplets, or larger aggregates of adhering vesicles were observed where a continuous outer membrane bounded the combined contents, nor were any discontinuous, double-bilayer diaphragms found. No nonspherical isolated vesicles were found whose enhanced area/volume ratio would reveal vesicle fusion. We conclude that little if any fusion has occurred at this stage. Fusion should be accompanied by some kind of bilayer perturbation. The high resolution images of all cleaved diaphragm areas, whether of the inner or outer monolayer, were as smooth as the outer portion of the vesicles, and thus revealed no structural perturbations of the adhering bilayers.

Diaphragm formation presumably depends on bridging

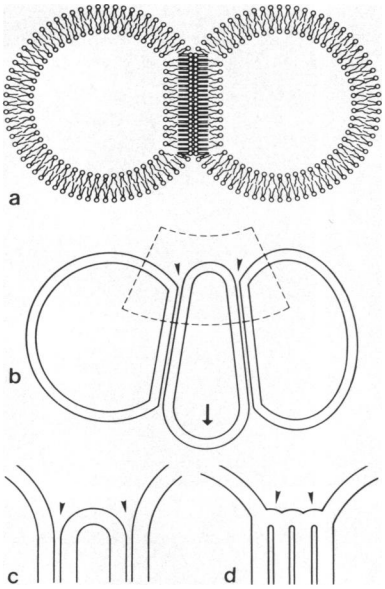

FIGURE 5 Hypothetical interactions between PS vesicles induced by $CaCl_2$. The formation of double membrane flat diaphragms at the area of contact (*a*) deforms participating vesicles (*b*, *c*). Vesicle breakage (at arrow *b*) and collapse explains the formation of the large ridges (Fig. 3 *a*). Calcium gaining access to the vesicle interior could result in its bridging interior halves of vesicle bilayers and in bilayer rearrangements such as fusion of the exoplasmic halves of neighboring vesicles (arrowheads *d*). This would explain the regular multilayer stacks of thin ridges (Fig. 4*b*).

adjacent bilayers by forming PS-Ca-PS complexes similar to those that ultimately comprise the stable multilamellar state (9, 10). These contacts represent a strong force of attraction between PS bilayers (21), on the order of 10 to 100 ergs/cm^2, sufficient to compete effectively with hydration repulsion (5). Such attraction leads to an increase in the area of contact between vesicles, deforming their spherical shape and stressing the bilayer membrane. Bilayers resist stretching and do rupture at 3% increase in area (22), a deformation approximately equivalent to that of the left-hand vesicle in Fig. 5 *b*. The attractive energy is so high that this degree of stretch is reached long before the adhered vesicles can form a stable configuration (21). The stress could be relieved in two major ways; either the diaphragm could break and the vesicles fuse, or the volume could be reduced by vesicle rupture or leak through the stressed bilayer. These considerations explain why these vesicles are eventually destroyed in $CaCl_2$ solutions and give rise to the complex morphology observed subsequent to simple vesicle adhesion.

The direct video observations show that both these stress-relieving events, either area or volume change, occur with GCV. The former, evidenced by diaphragm rupture, is not much more probable than the latter, suggesting that fusion is not a much more probable reaction to the stresses. This is so even though we estimate that the probability of rupture of a unit area of diaphragm is of the order of ten times that of nondiaphragmatic areas. The electron microscopy of the later transition stage suggests that the high curvature ridges are a consequence of these dynamic processes. The wider (50 nm) type of ridge can often be seen as the edge of a collapsed vesicle (Fig. 4 *c*) and we interpret them as such. The smooth cleavage faces along the multiple arrays of the narrower (20 nm) type of ridge may indicate that here the outer monolayers of adjacent vesicles have fused (arrowheads, Fig. 4 *b*). The high curvature of the narrower ridges is significant because it is greater than that of bilayer vesicles of the minimum attainable size (19), and would destabilize the bilayers in ways that could provide sites for fusion or partial fusion (12–14). The outer edges of the diaphragms could stress the external monolayers and promote their fusion. Such fusion would seal the diaphragms from $CaCl_2$, preventing their further growth. It remains to be explained why these multiple arrays of ridges are of equal length. We propose that their formation results from the rupture and total collapse of vesicles. Ca would gain access into the vesicle interior and cause adhesion of successive bilayers to the original diaphragm that might act as a template (Fig. 4 *d*).

Whether or not this interpretation of the more complex morphology of the later stages of the Ca-induced process is correct or complete, events during the early stages appear clear. We conclude that (*a*) the initial contact between vesicles results in the formation of large double-bilayer diaphragms causing major deformation of the spherical shape; (*b*) no morphological indication of bilayer destabilization could be detected; if present, it was either too small or short lived for the present methods of detection; (*c*) the reaction of adherent vesicles to the large stresses produced by their deformation is bilayer rupture, either at the diaphragm resulting in fusion or in the extra-diaphragm area resulting in vesicle rupture and leakage. The probability of diaphragm rupture was not so high as to make the fusion reaction predominant. Focusing or confining membrane instability to the contact area appears crucial to the control of the cellular process of fusion. We are seeking lipid and aqueous conditions, that might provide that focus of instability.

We would like to acknowledge both Adrian Parsegian's valuable suggestion of trying to synchronize and time events by rapid mixing and Bob Berger's help in accomplishing this through the use of his design of a ball mixer.

R. P. Rand is supported by the Natural Science and Engineering Research Council of Canada and is grateful for the expert assistance of Nola Fuller.

Received for publication 18 June 1984 and in final form 23 October 1984.

REFERENCES

1. Palade, G. E., and R. R. Bruns. 1986. Structural modulations of plasmalemmal vesicles. *J. Cell Biol.* 37:633–649.
2. Heuser, J. E., T. S. Reese, M. J. Dennis, Y. Jan, L. Jan, and L. Evans. 1979. Synaptic vesicle exocytosis captured by quick freezing and

correlated with quantal transmitter release. *J. Cell Biol.* 81:275–300.

3. Pinto da Silva, P., and B. Kachar. 1980. Quick-freezing vs. chemical fixation: Capture and identification of membrane-fusion intermediates. *Cell Biol. Int. Rep.* 4:625–640.
4. Ornberg, R. L., and T. S. Reese. 1981. Beginning of exocytosis captured by rapid-freezing of *Limulus* amebocytes. *J. Cell Biol.* 90:40–54.
5. Rand, R. P. 1981. Interacting phospholipid bilayers: Measured forces and induced structural changes. *Annu. Rev. Biophys. Bioeng.* 10:277–314.
6. Wilschut, J., N. Duzgunes, R. Fraley, and D. Papahadjopolous. 1980. Studies on the mechanism of membrane fusion: kinetics of calcium ion induced fusion of phosphatidylserine vesicles followed by a new assay for mixing of aqueous vesicle contents. *Biochemistry.* 19:6011–6021.
7. Wilschut, J., N. Duzgunes, K. Hong, D. Hoekstra, and D. Papahadjopoulos. 1983. Retention of aqueous contents during divalent cation-induced fusion of phospholipid vesicles. *Biochim. Biophys. Acta.* 734:309–318.
8. Rand, R. P., and S. Sengupta. 1972. Cardiolipin forms hexagonal structures with divalent cations. *Biochim. Biophys. Acta.* 255:484–492.
9. Portis, A., C. Newton, W. Pangborn, and D. Papahadjopolous. 1979. Studies on the mechanism of membrane fusion: Evidence for an intermembrane Ca^{+}-phospholipid complex, synergism with Mg^{2+} and inhibition by spectrin. *Biochemistry.* 18:780–790.
10. Loosley-Millman, M. 1980. Effects of ions on measured electrostatic repulsive forces between changed phospholipid bilayers. Ph.D. thesis, Guelph University, Guelph, Canada. 273 pp.
11. Verkleij, A. J., C. Mombers, J. Leunissen-Bijvelt, and P. Ververgaert. 1979. Lipidic intramembraneous particles. *Nature* (*Lond.*). 279:162–163.
12. Hui, S. W., and T. P. Stewart. 1981. Lipid particles are intermembrane attachment sites. *Nature* (*Lond.*). 290:427–428.
13. Miller, R. G. 1980. Do 'lipidic particles' represent intermembrane attachment sites? *Nature* (*Lond.*). 287:166–167.
14. Rand, R. P., T. S. Reese, and R. G. Miller. 1981. Phospholipid bilayer deformations associated with interbilayer contact and fusion. *Nature* (*Lond.*). 392:237–238.
15. Bearer, E. L., N. Duzgunes, D. S. Friend, and D. Papahadjopolous. 1983. Fusion of phospholipid vesicles arrested by quick-freezing. The question of lipidic particles as intermediates in membrane fusion. *Biochim. Biophys. Acta.* 693:93–98.
16. Miller, D. C., and G. P. Dahl. 1982. Early events in calcium-induced liposome fusion. *Biochim. Biophys. Acta.* 689:165–169.
17. Inoué, S. 1981. Video image processing greatly enhances contrast, quality, and speed in polarization-based microscopy. *J. Cell Biol.* 89:346–356.
18. Allen, R. D., and N. S. Allen. 1983. Video-enhanced microscopy with a computer frame memory. *J. Microsc.* (*Oxf.*). 129:3–17.
19. Szoka, F. C., and D. Papahadjopolous. 1978. Procedure for preparation of liposomes with large internal aqueous space and high capture by reverse-phase evaporation. *Proc. Natl. Acad. Sci. USA.* 75:4195–4198.
20. Papahadjopolous, D., W. J. Vail, K. Jacobson, and G. Poste. 1975. Cochleate lipid cylinders: Formation by fusion of unilamellar lipid vesicles. *Biochim. Biophys. Acta.* 394:483–491.
21. Parsegian, V. A., and R. P. Rand. 1983. Membrane interaction and deformation. *Ann. NY Acad. Sci.* 416:1–12.
22. Evans, E., and V. A. Parsegian. 1983. Energetics of membrane deformation and adhesion in cell and vesicle aggregation. *Ann. NY Acad. Sci.* 416:13–33.
23. Kwok, R., and E. Evans. 1981. Thermoelasticity of large lecithin bilayer vesicles. *Biophys. J.* 35:637–652.
24. Kendall, D. A., and R. C. MacDonald. 1982. A fluorescence assay to monitor vesicle fusion and lysis. *J. Biol. Chem.* 257:13892–12895.